

Sixth Quarterly Progress Report
NO1-DC-6-2111
**The Neurophysiological Effects of
Simulated Auditory Prosthesis
Stimulation**

C.A. Miller, P.J. Abbas, J.T. Rubinstein, B.K. Robinson and A.J. Matsuoka

Departments of Otolaryngology - Head and Neck Surgery,
Speech Pathology & Audiology and Physiology & Biophysics
The University of Iowa, Iowa City, IA 52242

April 30, 1998

Contents

1	Introduction	1
2	Summary of activities in the sixth quarter	1
3	Response properties of electrically stimulated auditory nerve fibers	2
3.1	Group trends - Threshold, Latency, Jitter, and Relative Spread	3
3.2	Relationship of single-fiber and EAP dynamic ranges	7
3.3	Derived EAP response from single-unit histograms	10
3.4	Adaptation	12
4	Preliminary results of ongoing work	15
4.1	An estimate of conduction velocity	16
4.2	Responses of single fibers to stimulation at different intra-cochlear sites	19
4.3	Effects of stimulus waveform morphology	19
5	Plans for next quarter	23
A	Presentations given during this reporting period	26
B	Publications in press	26
C	Manuscripts submitted	27

1 Introduction

The purpose of this contract is to investigate issues involving the transfer of information from implantable auditory prostheses to the central nervous system of individuals using these devices. This investigation is being pursued along multiple parallel tracks and include the use of animal experiments and computer model simulations to:

- Characterize fundamental spatial and temporal properties of intracochlear stimulation of the mammalian auditory nerve.
- Evaluate the use of novel stimuli and electrode arrays.
- Evaluate proposed enhancements in animals with a partially degenerated auditory nerve.

In this sixth Quarterly Progress Report, we focus primarily on the first two of these three aims. We begin with a presentation of analyses of single-fiber response properties to pulsatile stimulation. Preliminary single-fiber data were presented in the 3rd QPR; in this report, we present more detailed analyses and extensions of that earlier work. In addition to presenting group data on basic single-unit response properties, we also touch upon some issues of how single-fiber responses relate to the electrically evoked compound action potential (EAP). Finally, we present some preliminary results of ongoing experimentation involving conduction velocity, channel interaction and the use of pseudomonophasic stimuli.

2 Summary of activities in the sixth quarter

In our sixth quarter (January through March, 1998), the following activities related to this contract were completed:

- Additional EAP data were collected from 2 cats and 5 guinea pigs. The guinea pigs experiments focused on measuring responses to modulated pulse trains, high-rate pulse trains, and pulse trains in the presence of added gaussian noise. Single-fiber data were collected from one cat.
- Three presentations of work done under this contract were presented at the 21st Midwinter Meeting of the Association for Research in Otolaryngology (see Appendix A for the titles of the abstracts).

- A manuscript describing the characteristics of the EAP obtained from guinea pigs and cats was revised per peer-review and accepted for publication. Refer to Appendix B for citation information for this publication.
- A manuscript describing “psuedospontaneous activity,” the topic of the last QPR, was submitted to Hearing Research (see Appendix C).
- A new current source with improved bandwidth was breadboarded and tested, with successful results, on an animal preparation. This source will be used in upcoming parametric experiments of triphasic stimuli.
- Considerable effort was spent on off-line analysis of single-fiber data collected during the previous quarter.
- Began writing a manuscript focusing on single-fiber responses from cats.
- Began pilot work on the systemic deafening of guinea pigs for the phase of study involving chronically deafened guinea pigs.
- Completed analysis of histopathology in cats implanted chronically with the Advanced Bionics compartmental electrode.

3 Response properties of electrically stimulated auditory nerve fibers

As of the end of this quarter, single-fiber data from 12 cats has been collected and analyzed. Methodology for these studies has been provided in QPR 1 and 3. While some additional single-fiber experiments are planned for the seventh quarter (to satisfy our requirements for a publishable corpus of data), we currently have data from 177 fibers, from which several inferences can be made. In this first part of our section on experimental results, we characterize single-fiber responses to single presentations of short-duration (i.e., 27 or 39 μs) monophasic pulses delivered through a monopolar intracochlear electrode positioned in the basal turn of the cochlea. Response properties include threshold, latency, jitter, and relative spread (a measure of the slope of the input-output function, see Verveen (1961) or QPR 3). Additionally, we present information on neural adaptation, which has been observed in most of our preparations. We should note that, in the following

data, two different stimulus pulse durations were used. Early studies used the relatively short duration pulse. We subsequently chose the longer pulse duration in order to more consistently achieve stimulus levels capable of eliciting a saturated EAP response. In collecting single-fiber input output functions, each stimulus was presented 100 times in order to compute estimates of firing efficiency (spikes per 100 presentations), mean latency, and jitter.

3.1 Group trends - Threshold, Latency, Jitter, and Relative Spread

In the following group analyses, we find it useful to compare basic response measures across cathodic and anodic stimulus polarities, as is explicitly done in Figures 1 and 2. By examining these within-fiber differences, we may combine data sets across animals that likely vary in absolute value across animals. Threshold data from all fibers are plotted in Figure 1. We have defined “threshold” as the stimulus current level required to yield a firing efficiency of 50%. Thresholds to anodic stimuli are plotted versus thresholds to cathodic stimuli; note that two different stimulus pulse durations were used, although there is only one datum per fiber. The data of the left panel of Figure 1 include many fibers that were unresponsive to anodic stimuli at the highest level tested. In those cases, each datum is marked by a dotted symbol indicating the highest anodic level tested. The data of the right panel includes only fibers for which both anodic and cathodic thresholds were obtained. The polarity effect on threshold is statistically significant for both 26.8 μs ($t=4.13$, $p=0.00015$) and 39 μs ($t=5.86$, $p<0.00001$) stimulus durations.

It has been hypothesized that intracochlear electrical stimuli can excite fibers at longitudinal sites that differ appreciably in their membrane electrical characteristics (e.g., van den Honert and Stypulkowski, 1984). In one version of this hypothesis, it is suggested that cathodic stimuli excite the most peripheral neural sites whereas anodic stimuli excite more central sites (Parkins, 1989). Based upon the anatomy of the peripheral nerve-fiber terminations, it is reasonable to expect that the most peripheral segment has relatively high capacitance and leakage current. According to the hypothesis, one would therefore predict relatively less efficient integration of cathodic current when compared to the integration of anodic stimuli. A comparison of the mean anodic and cathodic threshold (solid symbols in Figure 1) for the two stimulus pulse durations do not support that hypothe-

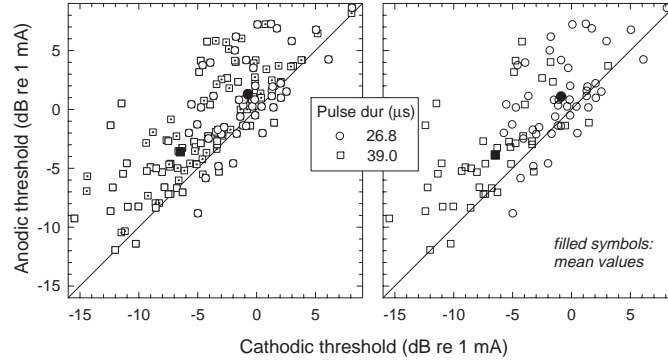


Figure 1: Single fiber thresholds to anodic monophasic stimuli plotted as a function of threshold to cathodic monophasic stimuli. The data were pooled from 12 cats. Over the course of those experiments, two stimulus pulse durations were used; only one datum is plotted per fiber. Mean data for each pulse duration are shown by the filled symbols. The left panel includes fiber data for which anodic threshold was not achieved at the highest level tested (symbols with small cross-hairs). The right panel includes only data from fibers in which thresholds to both polarities were achieved.

sis. As indicated by the changes in threshold across the two pulse durations, cathodic stimuli are integrated with efficiency comparable to that occurring with anodic stimulation.

Single-fiber latency, jitter, and relative spread (RS) data are presented for all fibers in the graphs of Figure 2. Note that latency is expressed as the mean spike latency (measured at the peak of the action potential relative to stimulus onset) at a firing efficiency of 50%. Similarly, jitter (the standard deviation of latencies) is also expressed as the value obtained at 50% firing efficiency. The six panels on the left portion of Figure 2 show the above measures from all 12 cats plotted as a function of stimulus level; panels of the right column plot the same dependent measures obtained with anodic stimuli versus the values obtained with cathodic stimuli.

The group latency data indicate a strong trend for relatively greater cathodic latencies, again as was suggested in our earlier report. Mean cathodic latencies to the 26.8 and 39 μ s pulses were 0.61 and 0.66 ms, respectively; mean anodic latencies were 0.44 and 0.47 ms, respectively. The across-polarity latency differences are significant at both stimulus durations (26.8 μ s: $t=11.0$, $p<0.00001$; 39 μ s: $t=8.03$, $p<0.00001$). Future refinement of

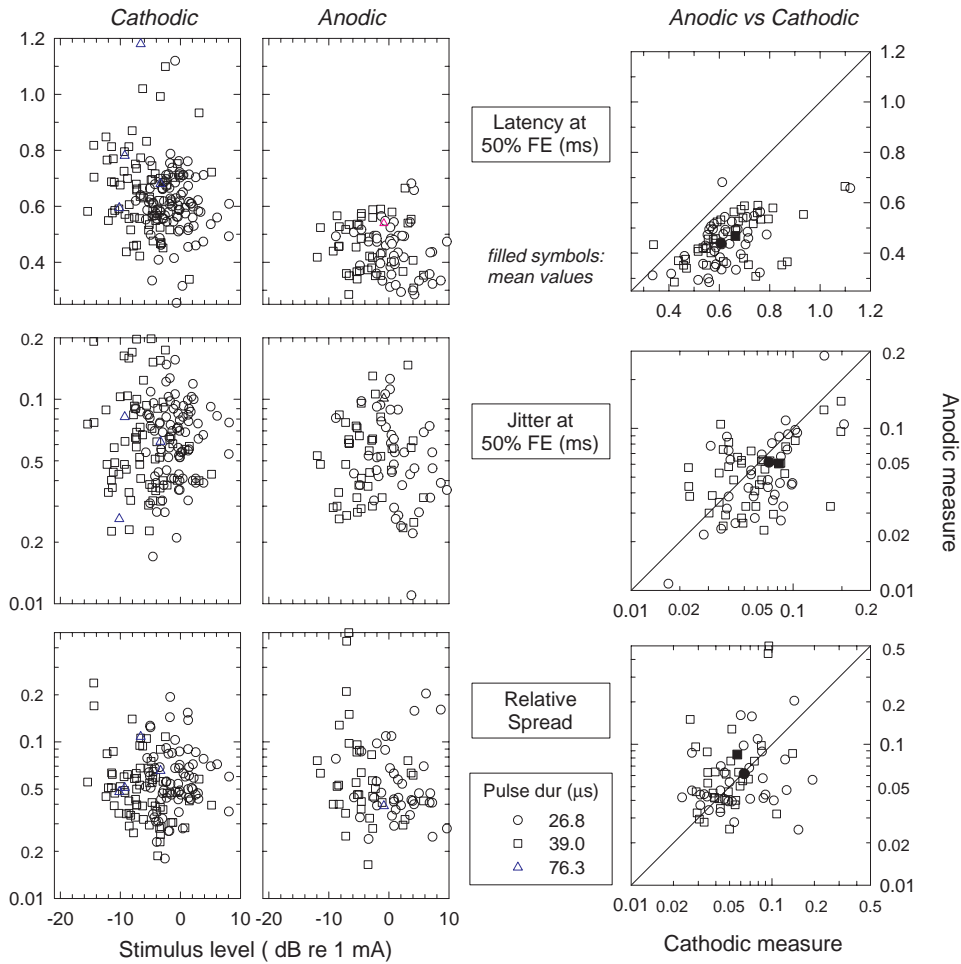


Figure 2: Summary of single-fiber latency, jitter, and relative spread (RS) data from 177 single fibers of 12 cats. These three measures are plotted versus stimulus level in the left two columns for cathodic and anodic stimulus pulses. The effects of stimulus polarity are more readily seen by the three graphs in the right column, where each of the measures obtained with anodic stimuli are plotted versus the same measure obtained with cathodic stimuli. Mean values at each stimulus pulse duration are plotted with filled symbols.

nerve-fiber models may result in application of these latency data to hypotheses dealing with putative sites of excitation. For example, these data may be compared with models producing both dendritic and axonal excitation modes, to determine whether the polarity-dependent latency shifts are consistent with those two modes of excitation. Alternately, future experimental animal work, with more focused and site-selective stimulation, may also address such issues.

Group jitter data are presented in the middle row of graphs of Figure 2. The mean values for jitter for 26.8 and 39 μ s pulses with cathodic stimulation are 0.071 and 0.082 ms, respectively. For anodic stimuli, the mean values are 0.062 and 0.061 ms, respectively. In our results in QPR 3, we were unable to resolve any effect of stimulus polarity on jitter (again, measured at 50% firing efficiency). In our present data, paired t-tests for each stimulus pulse duration fail to reach significance (26.8 μ s: $t=1.44$, $p=0.157$; 39 μ s: $t=1.28$, $p=0.205$). When the data are combined across the two pulse durations, however, a significant effect is obtained ($t=2.23$, $p=0.0286$). Combining the data from the two polarities is justified by the fact that each fiber contributes only one datum for each stimulus polarity. Note that additional data collection planned for the next quarter will add to statistical power to the present data set.

Greater cathodic jitter is consistent with two different theoretical notions. The first invokes a hypothesis that the site of excitation for cathodic stimuli is intrinsically noisier than the anodic site, resulting in greater temporal uncertainty for cathodic stimulation. This notion implies that the two excitation sites have fundamentally different membrane properties. A second notion is that increased jitter caused by either propagation through intrinsically noisy nodes of Ranvier or propagation through the cell body can account for relatively greater cathodic without any differences in the membrane properties at the two excitation sites. Model simulations suggest that propagation through the cell body results in greater increase in jitter than does that contributed by propagation through nodes alone (Rubinstein and Dynes, 1993). Future model work will be directed to resolve which combination of these hypotheses is most appropriate in the case of intracochlear stimulation of the auditory nerve.

Finally, values of RS are shown in the bottom scatter plots of Figure 2. Mean RS values for 26.8 and 39 μ s pulses with cathodic stimulation are 6.4 and 5.7%, respectively; for anodic stimuli, the mean RS values are 6.2 and 8.4%. Paired t-tests fail to indicate any polarity effects, even when the RS data are pooled across the different pulse durations. Assuming that RS is a

property of the membrane at the site of excitation (Rubinstein and Dynes, 1993), polarity-dependent differences in RS would reflect different membrane properties at the anodic and cathodic sites of excitation. The data presented here do not support the hypothesis that the anodic and cathodic sites differ appreciably in their stochastic membrane properties.

Figure 3 presents an analysis of the temporal firing properties of single fibers for both cathodic and anodic stimulation. The mean latency (top panels) and jitter (bottom panels) of 51 fibers from 6 cats are plotted as functions of firing efficiency. In computing the mean and median plots (filled symbols), each fiber's data was fit to either a first- or third-order regression line to provide estimates of each function's values at standard values (i.e, 5, 10, 15%, etc.) of firing efficiency. These estimated values were then averaged across fibers to obtain the mean and median values. Note that, relative to the anodic data, the mean cathodic latency data is skewed somewhat by the presence of a few fibers with relatively large mean latencies. These long-latency fibers also undergo, relative to the average fiber, greater decrements in latency with increasing firing efficiency. This group of fibers in the cathodic data may be indicative of a minority of fibers that are excited along the unmyelinated segment of the distal neural processes, a putative mode of excitation with cathodic stimuli. Finally, note that the change in latency with increases in firing efficiency is greater with cathodic stimulation than it is with anodic stimulation, suggesting that the cathodic site of excitation undergoes a relatively greater shift in position. Also, relatively larger latency decrements occur at high levels of firing efficiency.

3.2 Relationship of single-fiber and EAP dynamic ranges

An issue relevant to the development of accurate computational models involves the distribution of single-fiber thresholds with electrical stimulation. An experimental approach to this question would entail the collection of a representative survey of single-fiber thresholds from a single cat. As of this writing, our the largest data set comprises 27 fibers. In Figure 4 (left panel), we present single-fiber thresholds from all cats yielding data from at least 10 fibers. Note that, beginning with subject C31, stimulus pulse duration was changed from 26.8 to 39 μ s, accounting for the lower thresholds from the later subjects. For each cat, a vertical bar indicates the range of fiber thresholds. Across the seven cats, the range of thresholds varies from 6.1 to 13.5 dB. Threshold histograms for the two cats yielding the most single-fiber threshold data are plotted in the right column of the figure. Note that it

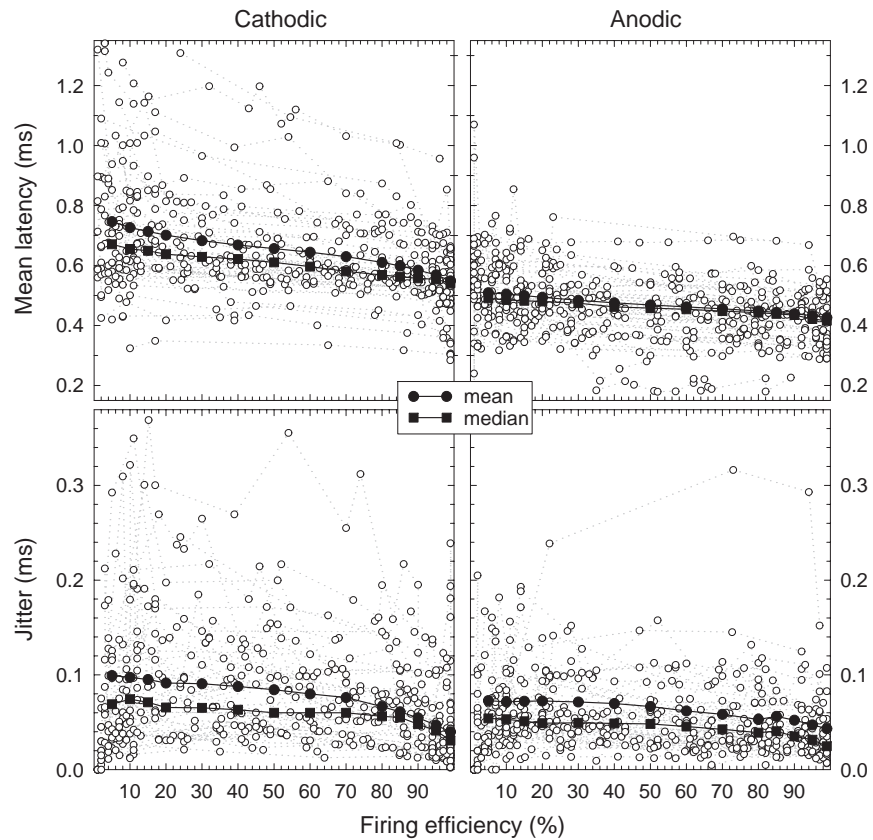


Figure 3: Single-fiber mean latency and jitter for cathodic and anodic stimuli plotted as a function of firing efficiency for 51 fibers of 6 cats. Monophasic stimulus pulses of either $26.8 \mu\text{s}$ or $39 \mu\text{s}$ duration were used. Mean latency and jitter functions are shown by the filled circles; median data are shown by the filled squares. In order to give each fiber equal weight in the mean and median measures, each fiber's data were fit to curves to provide estimates of latency and jitter at each standard value of firing efficiency.

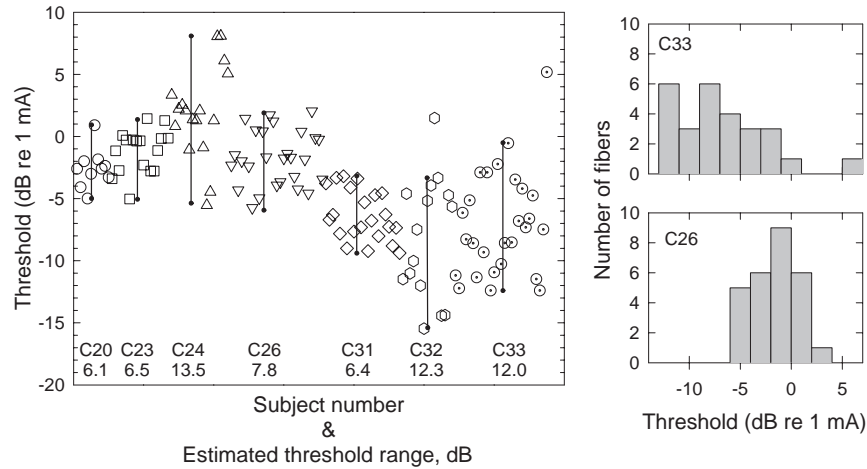


Figure 4: Estimates of the range of single-fiber thresholds for each of seven cats. The vertical lines in the graph of the left panel indicate each threshold range, excepting, in two cases, points deemed to be outliers. The ranges covered by each line segment are listed (in dB) at the bottom of the graph. Threshold histograms for the two cats with the most data are shown at right.

is difficult to estimate the threshold distribution function with such limited data sets. Collection of a large set of fiber threshold data from one animal in order to better specify the threshold distribution function is among future goals.

A related issue of concern to modeling efforts is a description of the relationship between the threshold range of single-fibers and the dynamic range of the gross neural (i.e., EAP) response. In Figure 5, the seven single-fiber threshold ranges of the previous figure are plotted along with the dynamic ranges of EAP amplitude-level functions obtained from 11 cats. The EAP amplitude levels at 5% and 95% of the maximum (saturation) level were used to compute EAP dynamic range. Note that, while there is appreciable variability across subjects, both the single-fiber and gross-potential indices of dynamic range cover similar ranges. It is worth noting that the average single-fiber RS values reported above correspond to 5-95% dynamic ranges between 1.1 and 1.7 dB, considerably smaller than the average EAP value of 10 dB obtained from the cats of Figure 5.

A good understanding of the relationship between single-fiber responses

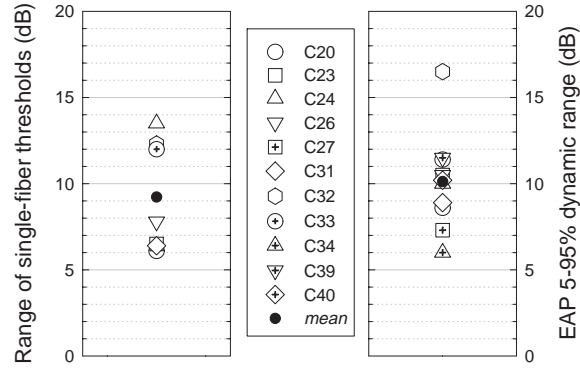


Figure 5: A comparison of the range of single-fiber thresholds of 7 cats (left panel) and the dynamic range of EAP amplitude-level functions of 11 cats (right panel). The single-fiber data are those from Figure 4. The EAP dynamic range values were defined by the 5% and 95% amplitude points from each cat’s amplitude-level function; 100% was defined by the saturation (maximum) amplitude of each EAP function.

and the EAP dynamic range is critical for accurate modeling of the gross neural response. This is shown schematically in the plots of Figure 6. If, as in “Model 1”, the dynamic range (or RS) of the underlying single fibers is comparable to that of the EAP amplitude-level function, there must be a relatively narrow distribution of single-fiber thresholds. In this case, the shape of the EAP amplitude-level function is largely determined by that of the single fibers. However, in “Model 2”, where the EAP dynamic range is much greater than that of the underlying fibers, the single-fiber threshold distribution function plays a greater role in determining the EAP function than does the exact form of the single-fiber functions. The data we present here suggests that the latter condition holds, implying that the development of an accurate fiber threshold distribution is critical to the accurate modeling of the EAP.

3.3 Derived EAP response from single-unit histograms

A preliminary attempt to derive the EAP response from underlying single-fiber activity has been performed using data from one cat. EAP amplitude-level and 24 single-fiber input-output functions obtained from the same cat are shown in Figure 7 for both stimulus polarities. This comparison clearly

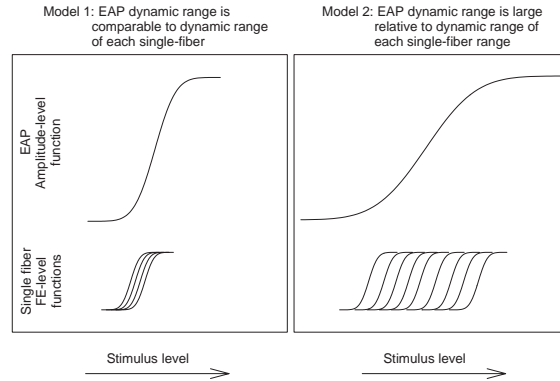


Figure 6: Two models of possible relationships between EAP input-output functions and underlying single-fiber functions. In Model 1, single-fiber and EAP dynamic ranges are comparable, requiring a narrow distribution of single-fiber thresholds. Model 2 has a wider range of single-fiber thresholds, resulting in a relatively large dynamic range for the EAP amplitude-level function.

demonstrates the large difference in EAP and single-fiber dynamic ranges, as was discussed above. Referring to our models of Figure 6, this experimental data better fits “Model 2” than it does “Model 1”. As is typical in our preparations, cathodic stimuli evoked responses in more fibers than did anodic stimuli; thus, the EAP was derived for the case of cathodic stimulation. The derived EAP was computed by the convolution of a unitary neural response with the composite PST histogram computed at various stimulus levels (Goldstein and Kiang, 1958; Goldstein, 1960). In our work, we have not recorded the unitary response. Instead, for this derivation, we computed it from the deconvolution of the high-level EAP with the corresponding high-level composite histogram.

Representative derived and actual EAP waveforms are shown in Figure 8 (left panels), along with their respective latency-level and amplitude-level functions (right panels). Note that both derived functions are shifted to higher stimulus levels, presumably due to undersampling of the population of nerve fibers. Also, note that the derived latency-level function fails to reach the minimum latency achieved by the actual EAP waveform. This discrepancy is due, in part, to our inability to accurately record single-fiber waveforms at high stimulus levels, in the presence of appreciable artifact from the gross neural response. Nonetheless, the derived data approximate

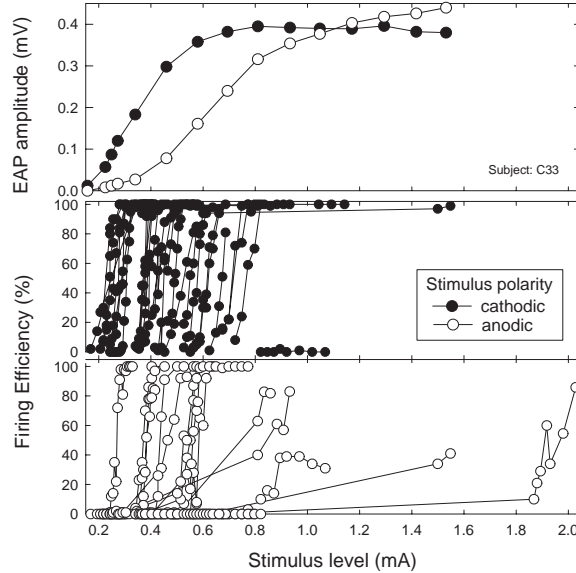


Figure 7: EAP amplitude-level and single-fiber FE-level functions obtained from a cat (C33) for monophasic cathodic and anodic stimuli.

the general shape of the latency-level function, as well as the dynamic range of the EAP amplitude-level function.

3.4 Adaptation

In QPR 3, we noted that some fibers undergo adaptation in manner dependent upon stimulus polarity. In this reporting period, we have obtained additional measures of adaptation phenomena. We estimate that roughly 10% of surveyed fibers show adaptation to anodic stimulation during the course of data collection. Figure 9 illustrates adaptation occurring in two different single fibers over the course of several minutes of stimulation. We note that our standard search and data acquisition pulses are presented with an interpulse interval (IPI) of at least 30 ms; in the data presented in Figure 9, an IPI of 45 ms was used. Note that, in both cases, the fibers are initially more responsive to anodic stimulation than they are to cathodic stimulation. Over the course of several minutes, the anodic response undergoes a relatively large degree of adaptation. In contrast, fibers respond in a relatively stable manner under cathodic stimulation. Although one of the two fibers shown in Figure 9 demonstrates adaptation to cathodic stimulation, that is

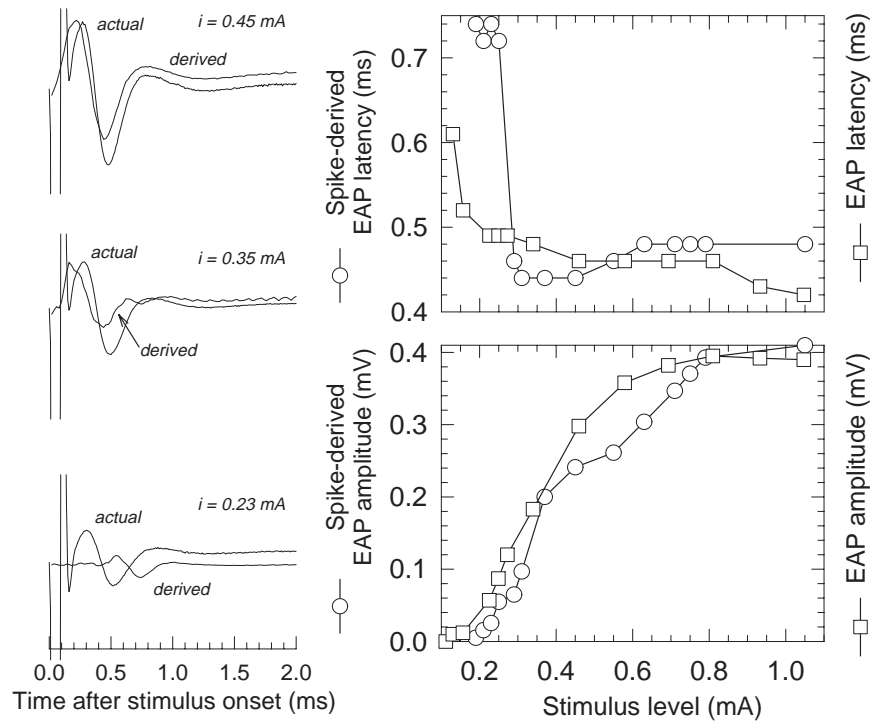


Figure 8: A comparison of actual and derived EAP responses for cat C33. The derived waveforms (left panels) were computed by convolving the composite PST histogram (comprised of the 24 fibers shown in Figure 7) with an estimate of the "unitary response" (see text). Latency-level and amplitude-level functions for both the derived and actual EAP responses are shown in the right panels.

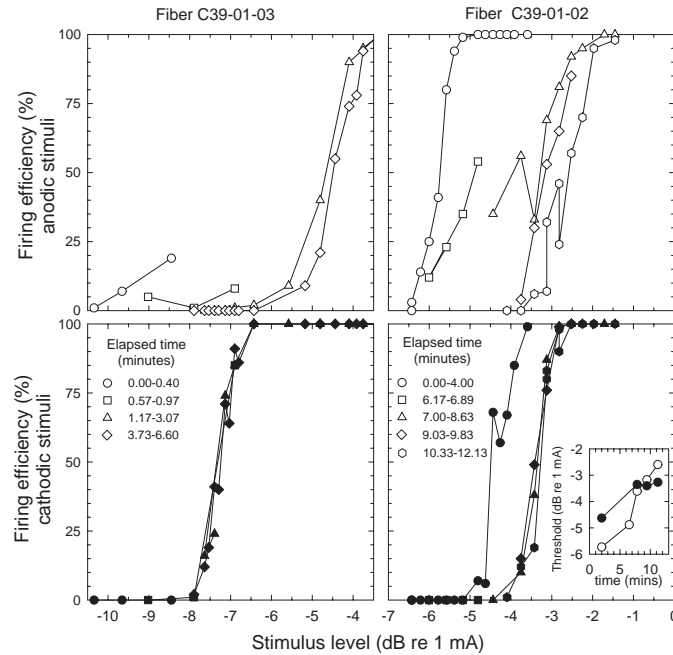


Figure 9: Examples of polarity-dependent adaptation observed in a minority of fibers. In both cases shown, the fibers were initially more sensitive to anodic stimuli, then adapted to the typical pattern of greater sensitivity to cathodic stimuli. Fiber C39-01-02 (right panels) undergoes adaptation to cathodic stimuli, but a lesser degree, as illustrated by the small inset plot.

a relatively rare phenomenon. This pattern of adaptation is in some cases, but not all, related to IPI, as is illustrated in Figure 10. In this case, the fiber is stimulated at a single current level over the course of two minutes of data collection. The responses to anodic stimuli at an IPI=30 ms adapt at a relatively constant rate and then recover to almost the initial value within an interval of about one minute.

We are unaware of any previous investigation of this phenomenon, although van den Honert and Stypulkowski (1984) reported observing upward threshold shifts shortly after onset of stimulation in some units. Other investigators have noted that the auditory nerve can be relatively unresponsive to one phase of sinusoidal stimuli (van den Honert and Stypulkowski, 1987; Dynes and Delgutte, 1992), consistent with adaptation and threshold shift affecting primarily anodic stimulation. It is not surprising that there is scant

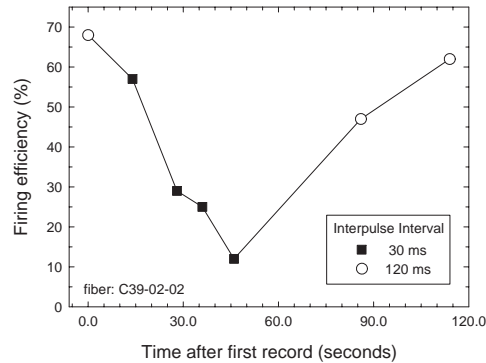


Figure 10: Plot of repeated measures of firing efficiency with fiber demonstrating adaptation. Constant-level, stimulus pulses were presented at two different rates, as indicated by the two interpulse intervals. Reductions in FE occurring at the higher rate were reversed by presenting stimuli at a lower rate. Data shown are for anodic stimuli.

report of this effect, given that most previous studies employed biphasic stimuli and the response to cathodic stimuli is generally stable. The mechanism of this effect is puzzling. Javel (1987) has shown that auditory fibers can sustain much higher discharge rates than are elicited by our relatively slow trains of pulses. Upward shifts in threshold were also observed by Pousart (1965), who studied single-fiber responses to electrical stimulation in the sciatic nerve of frog. He speculated that the phenomenon may have been related to fiber injury or a slow change in resting membrane potential. In one case, we demonstrated that reductions in firing efficiency can be reversed by increasing IPI (e.g., Figure 10) and cannot simply be attributed to contact injury. The existence of a polarity dependent adaptation phenomenon may provide a rationale for the application of pseudomonophasic stimulus pulses. If this adapting effect could occur in humans with cochlear implants, it may be advisable to avoid stimuli that could result in such unpredictable, transient effects.

4 Preliminary results of ongoing work

In addition to the results reported above, we have collected preliminary data related to several other issues outlined in the original contract proposal during this reporting period.

4.1 An estimate of conduction velocity

Experimental estimates of action potential conduction velocity would contribute to accurate models and predictions of responses from the auditory nerve. Figure 11 illustrates results from our first EAP measurements designed to estimate the conduction velocity along the central portion of auditory nerve. This experiment was conducted on a preparation that provided relatively generous exposure (up to 2 mm) of the length of the auditory nerve. The recording electrode micromanipulator was aligned parallel to the longitudinal course of the nerve as illustrated schematically in the figure. The recording ball electrode was then placed at five different positions along the length of the nerve (as measured by a micrometer stage) and EAP growth functions measured at each position. The amplitude for both anodic and cathodic stimulation varied across recording position as illustrated in the lower two graphs. The waveform for all five recording positions showed clear N1 and P2 peaks. As expected, the latency of the peaks varied with recording positions, presumably due to the propagation of action potentials.

Calculated conduction velocities based on the data in Figure 11 are plotted as a function of stimulus level in Figure 12. Conduction velocities were calculated only on the basis of latency differences obtained at the extreme ends of the five recording sites shown in Figure 11. Estimates based on N1 and P2 latencies yielded slightly different, but generally overlapping, values of conduction velocity. The mean values plotted across all estimates for this animal yield values ranging from 14 to 17 m/s. Anatomical surveys have estimated the diameter of the myelinated central axons to be between 2 and 4 μm (Arnesen and Osen, 1978; Liberman and Oliver, 1984). Estimates of conduction velocity based upon fiber diameter (Hursh, 1939; Burgess and Perl, 1973) yield velocities consistent with this preliminary estimate.

Several qualification to the above measurements should be noted. Errors in our alignment of the micromanipulator axis parallel to the nerve fibers would result in over-estimation of the conduction velocity. Nerve fibers within the nerve trunk do not follow a linear course, but rather spiral somewhat (Sando, 1965, Arnesen and Osen, 1978). These curved paths will result in underestimation of velocity, since we have made linear distance measures. Finally, the amplitude of the response varies across recording positions, suggesting a difference in the distance from the recorded site across recording electrode position. These issues will be investigated further as these measures are verified in future experimental subjects.

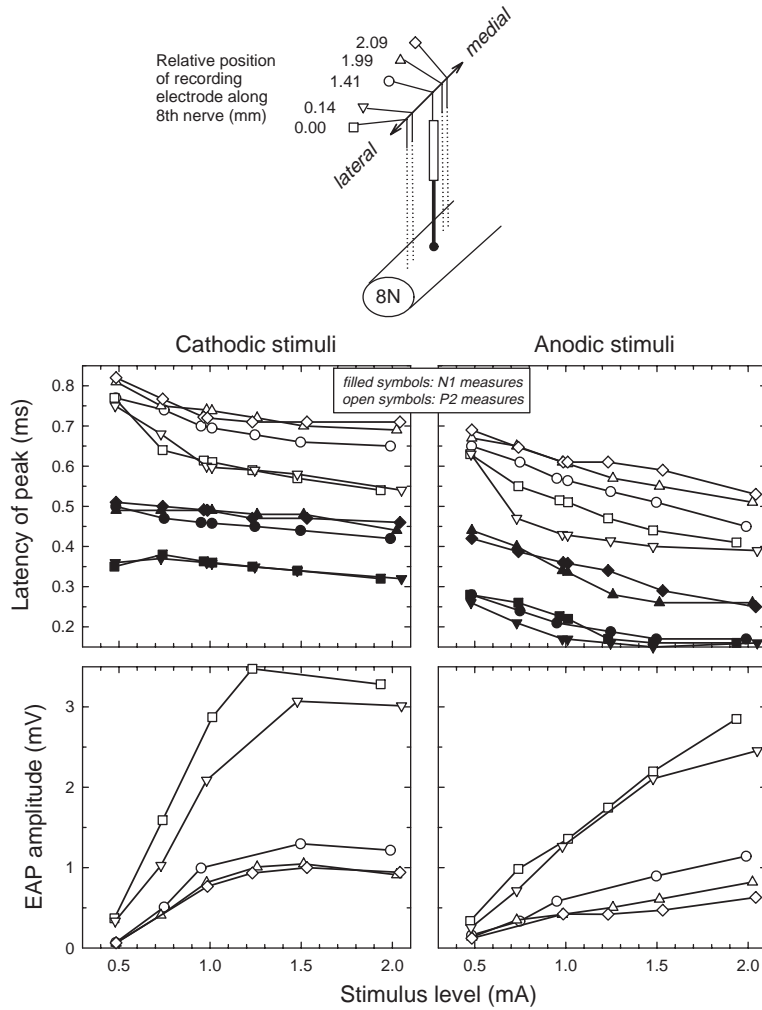


Figure 11: EAP latency-level (top graphs) and amplitude-level (bottom graphs) functions obtained at 5 different recording sites along the lateral-distal axis of the auditory nerve of a cat. The schematic drawing at the top of this figure shows the relative positions of the recording electrode used to obtain the input-output data.

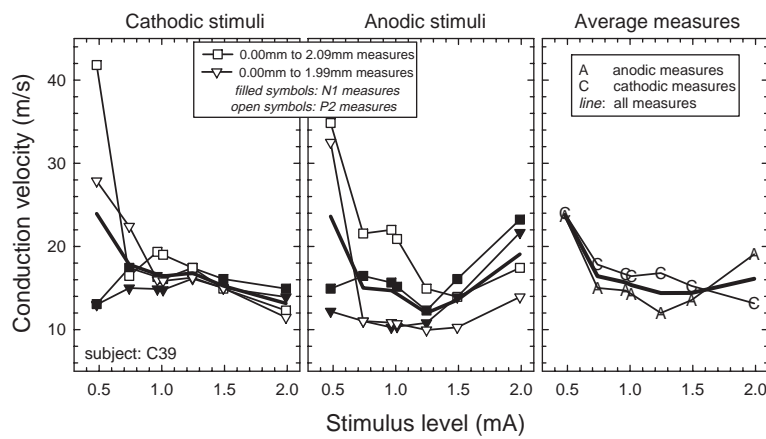


Figure 12: Preliminary estimates of auditory nerve conduction velocity using the data of the previous figure. All estimates are shown plotted as functions of stimulus level. Various estimates are shown for both cathodic (left panel) and anodic (middle panel) stimuli. Both the latencies of the N1 and P2 peaks were used and are plotted separately by filled and open symbols, respectively. Two sets of repeated measures were obtained by recording EAP input-output functions at a total of three different sites, as indicated in the legend. The graph of the right panel plots the average anodic, average cathodic, and overall average measures of conduction velocity.

4.2 Responses of single fibers to stimulation at different intracochlear sites

Another part of the proposed contract research was to investigate channel independence using a multi-electrode array similar to that used in cochlear implants in humans. We are currently making measures at both the single-fiber and gross-potential levels. Initial single-fiber input-output functions obtained with a USCF-Duke-type multi-contact array are shown in Figure 13. This array is designed to insert into the basal turn of the cat cochlea. In this experiment, four of the array's electrodes were used in monopolar configurations to stimulate single fibers. The longitudinal distance between each of the four chosen electrodes (designated 2, 4, 6, and 8 in the figure) is approximately 1 mm, with Electrode 2 the most apical of the four. While these results are preliminary, we can note some interesting trends. Clear differences in sensitivity across stimulating electrode are demonstrated, indicating that, at the single-fiber level, a degree of channel independence is possible. In at least two data sets of the fibers shown, there is greater independence among electrodes with cathodic stimulation. Furthermore, the most sensitive stimulating electrode varies across fibers, consistent with a hypothesis of "place" selectivity for each stimulating electrode. In some cases, the ordering of electrodes for sensitivity varies with stimulus polarity. As of this report, we have not seen any systematic change in single-fiber RS values as a function of stimulus electrode. Further experiments will examine these issues in both single fiber recordings as well as in channel interaction measures using the EAP.

4.3 Effects of stimulus waveform morphology

Most recordings reported in our QPRs to date have primarily used either monophasic or pseudomonophasic stimuli. During this reporting period, we also have begun making measurements using other stimulus waveforms. Since most cochlear implants use biphasic pulsatile stimulation, it is of interest to compare our monophasic data with responses to biphasic stimulation. Figure 14 illustrates recordings from four neurons in which we have measured response to both monophasic and biphasic stimuli. Response to both stimulus polarities are shown, in the case of biphasic stimuli polarity indicates that of the initial stimulus pulse. All four fibers show higher thresholds in response to biphasic stimuli. Cathodic stimuli tend to produce lower thresholds than anodic stimuli for both monophasic and biphasic stimuli.

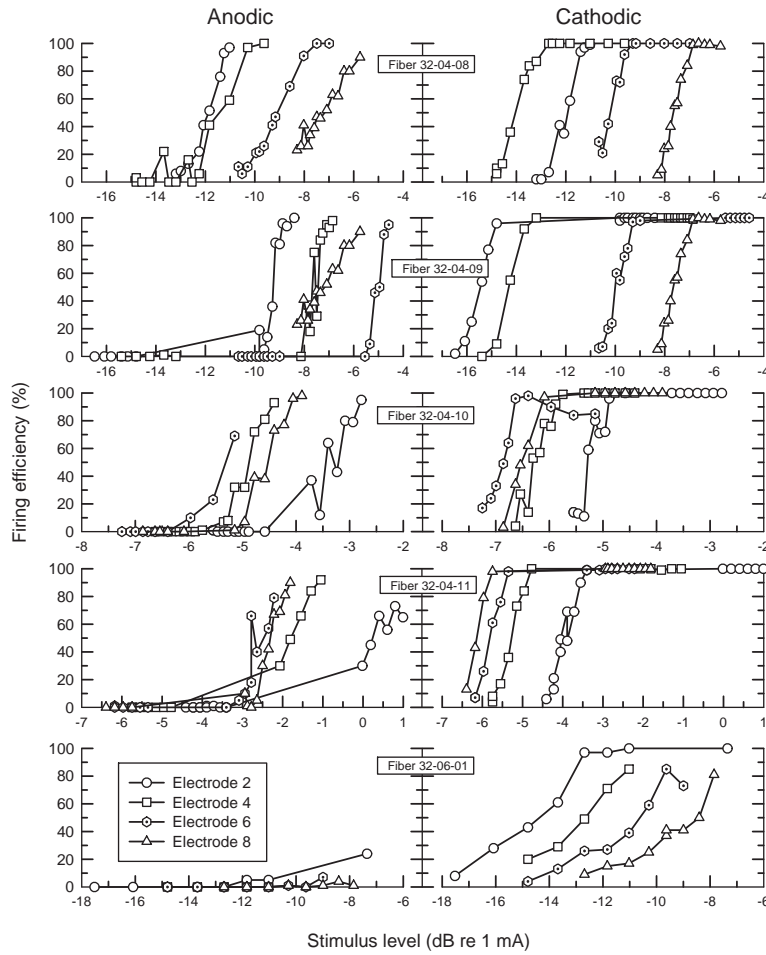


Figure 13: Input-output functions for 5 fibers obtained using the Duke-UCSF intracochlear array. Four electrodes of this array were used to stimulate at four different longitudinal sites. Electrode 2 is the most apical electrode; electrode 8, the most basal. Monophasic anodic (left panels) and cathodic (right panels) stimuli were delivered with each electrode serving as a monopolar source. Note that different decibel scales are used across fibers.

The difference between cathodic and anodic threshold is markedly greater for monophasic stimuli. Fiber C39-01-04 (lower left panel) showed no response to anodic stimulation over the range of the current source. These observations are consistent with the notion that, with either monophasic or biphasic stimulus pulses, the cathodic phase of the pulse is the effective stimulus. In two fibers, C26-06-03 and C40-03-06 (right panels), cathodic, monophasic stimulation resulted in significantly greater RS than for biphasic stimuli. One possible explanation for such differences is the effect of second phase on the nerve membrane properties. Such stimulus-related differences in RS were not observed in all nerve fibers, however.

An analysis of the slopes of EAP growth functions in 11 animals shows no consistent difference in the slope (of the linear portion of the amplitude-level function) calculated for monophasic and biphasic stimuli (Figure 15). Based on the above discussion of EAP and single-fiber dynamic ranges, we might expect that changing RS in a small subpopulation of fibers may have relatively little effect on the overall EAP growth.

The effect of a second, anodic, phase on the response to the cathodic stimulus phase has been further investigated using EAP amplitude-level functions. Our "monophasic" stimuli are, in fact, delivered through a capacitively coupled current source with a relatively long (approximately 30 ms) time constant, so that there is a long charge recovery phase following the initial phase of stimulation. We have also used "pseudomonophasic" pulses in some experiments (many of those investigating the response to pulse trains) in order to more precisely control the period of charge recovery. In collecting the EAP data of Figure 16, we used pseudomonophasic pulses and varied the duration and level of second phase. The legend of the figure refers to the level of the initial (cathodic) pulse, which has a fixed duration of 39 μ s. On the abscissa is plotted the duration of the second (anodic) phase. In each case, the level of the second phase is adjusted for charge balance with the first phase. The shortest duration of 39 μ s is essentially a normal biphasic pulse. In the figure, EAP amplitudes for each stimulus level are normalized to the amplitude obtained at the longest (4000 μ s) anodic phase duration. At high stimulus levels (1.99 and 2.57 mA), there is relatively little change in response amplitude as duration of the second phase is decreased. It is worthy of note, however, that there appears to be an enhancement of the response amplitude at very low second pulse durations, consistent with our observation of a higher EAP saturation amplitude in some cases. At the lowest stimulus level, there is considerable decrease in response amplitude at durations as long as 1 ms, suggesting that recovery phase of 2 ms or may

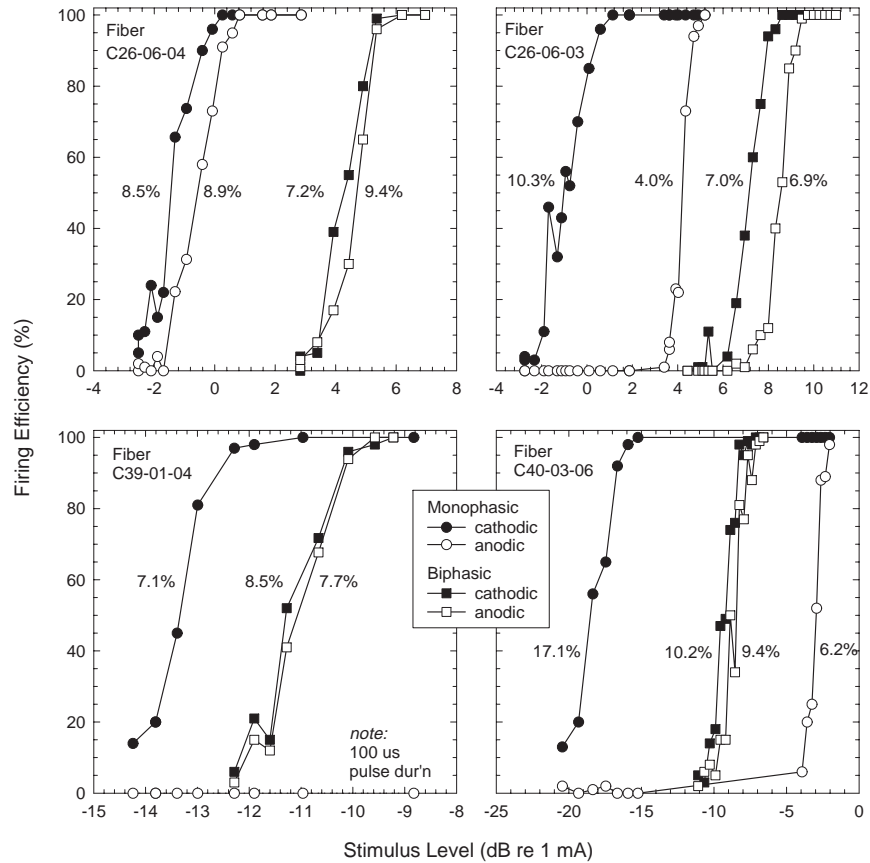


Figure 14: Input-output functions for 4 fibers using both monophasic and biphasic stimulus pulses. In 3 of the 4 cases, 39 μ s pulses were used; 100 μ s pulses were used in fiber C39-01-04 (lower left panel). Estimates of relative spread are shown (in %) next to each input-output function. Note that different decibel scales are used in each graph.

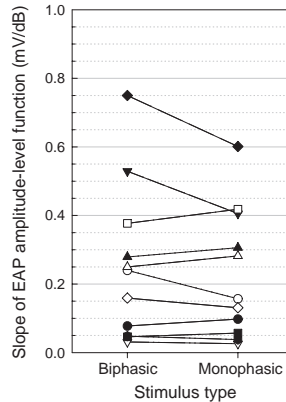


Figure 15: Comparison of EAP amplitude-level slopes obtained with biphasic and monophasic stimuli. Data from 11 cats are shown. The stimuli were cathodic monophasic pulses or a cathodic-first biphasic pulses; phase duration was $39 \mu\text{s}$ in both cases. Slope was calculated by linear regression (amplitude in mV units and current level in dB re 1 mA) over the linear portion of each amplitude-level function.

be necessary to negate the effects of the anodic phase on the response.

We plan in the next quarter to more systematically investigate the effects of stimulus waveform using both pseudomonophasic and triphasic stimuli to elicit EAP and single fiber responses.

5 Plans for next quarter

- Perform experiments on two more cat preparations to complete data collection for a manuscript on single-fiber responses.
- Complete data analysis and prepare a manuscript for publication, detailing basic properties single-fiber responses.
- Continue single unit and EAP experiments investigating channel interaction, propagation velocity, and stimulus waveform.
- Continue deafening guinea pigs for planned study of effects of neural degeneration on EAP responses during year 3 of the contract.
- Preparation of manuscripts related to EAP measurements in response to constant amplitude and amplitude modulated pulse trains.

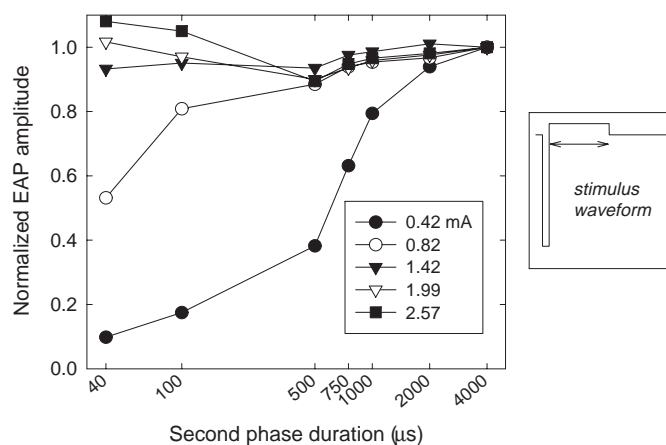


Figure 16: Effect of the duration of the second stimulus phase on the EAP response. For each plotted function, EAP amplitudes are normalized to the response obtained with a second phase duration of $4000 \mu\text{s}$. The stimulus, shown schematically in the right panel, consists of a cathodic phase followed by a charge-balancing anodic phase. The legend indicates the cathodic (first phase) current level. The abscissa corresponds to the duration of the second (anodic) phase duration, which was systematically varied.

References

- [1] Arnesen, A. R. and Osen, K.K. (1978). The cochlear nerve in the cat: topography, cochleotopy, and fiber spectrum. *J. Comp. Neur.* 178, 661-678.
- [2] Burgess, P.R. and Perl, E.R. (1973). Cutaneous mechanoreceptors and nociceptors. In *Handbook of Sensory Physiology, Vol. II, Somatosensory System*, A. Iggo (ed.), Springer-Verlag, Berlin.
- [3] Goldstein, M.H. (1960). A statistical model for interpreting neuroelectric responses. *Information and control* 3, 1-17.
- [4] Goldstein, M.H. and Kiang, N. Y.-S. (1958) Synchrony of neural activity in electric responses evoked by transient acoustic stimuli. *J. Acoust. Soc. Am.* 30, 107-114.
- [5] Hursh, J.B. (1939). Conduction velocity and diameter of nerve fibers. *Am. J. Physiol.* 127, 131- 139
- [6] Javel, E., Tong, Y.C., Shepherd, R.K., Clark, G.M. (1987). Responses of cat auditory nerve fibers to biphasic electrical current pulses. *Ann. Otol. Rhinol. Laryngol.* 96 (Suppl. 128) pp 26-30.
- [7] Liberman, M.C. and Oliver, M.E. (1984) Morphometry of intracellularly labeled neurons of the auditory nerve: correlations with functional properties. *J. Comp. Neurol.* 223, 163-176.
- [8] Parkins, C.W. (1989) Temporal response patterns of auditory nerve fibers to electrical stimulation in deafened squirrel monkeys. *Hear. Res.* 41, 137-168.
- [9] Poussart, D. J.-M. (1965) Measurements of latency distributions in peripheral nerve fibers. Master's Thesis, Massachusetts Institute of Technology.
- [10] Rubinstein, J.T. and Dynes, S.B.C. (1993). Latency, polarity and refractory characteristics of electrical stimulation: Models and single-unit data. *Abstracts of Assoc. Res. Otolaryngol.*
- [11] Sando, I. (1965) The anatomical interrelationships of the cochlear nerve fibers. *Acta Oto- laryng.(Stockh.)* 59, 417-436.

- [12] van den Honert, C. and Stypulkowski, P.H. (1984). Physiological properties of the electrically stimulated auditory nerve. II. Single fiber recordings. *Hear. Res.* 14, 225-243.
- [13] van den Honert, C. and Stypulkowski, P.H. (1987) Temporal response patterns of single auditory nerve fibers elicited by periodic electrical stimuli. *Hear. Res.* 29, 207-222.
- [14] Verveen, A.A. (1961). *Fluctuation in Excitability*, Drukkerij, Holland N.V., Amsterdam.

A Presentations given during this reporting period

Abbas, P.J., Matsuoka, A.J., McDougall, V.M., Miller, C.A., J.T. Rubinstein (1998). Compound action potential patterns in response to electrical amplitude-modulated pulse trains in the guinea pig auditory nerve. Abstract 287, Association for Research in Otolaryngology Midwinter Meeting 20, St. Petersburg Beach, FL.

Matsuoka, A.J., Abbas, P.J., Rubinstein, J.T., Miller, C.A. (1998). Compound action potential responses to constant electrical pulse trains: Effects of stimulus parameters on response pattern. Abstract 286, Association for Research in Otolaryngology Midwinter Meeting 20, St. Petersburg Beach, FL.

Miller, C.A., Abbas, P.J., Rubinstein, J.T., Robinson, B.K., and Matsuoka, A.J. (1998). Single-fiber and compound action potential recordings from cat auditory nerves using monophasic current pulses delivered through monopolar intracochlear electrodes. Abstract 285, Association for Research in Otolaryngology Midwinter Meeting 20, St. Petersburg Beach, FL.

B Publications in press

Miller, C.A., Abbas, P.J., Rubinstein, J.T., Robinson, B.K., Matsuoka, A.J., and Woodworth, G. (1998) Electrically evoked compound action potentials of guinea pig and cat: responses to monopolar, monophasic stimulation. *Hear. Res.* [tentative volume and pages: 119, 142-154]

C Manuscripts submitted

Rubinstein, J.T., Wilson, B.S., Finley, C.C. and Abbas, P.J. Pseudospontaneous activity: stochastic independence of auditory nerve fibers with electrical stimulation.